Interplay between electron correlations and polar displacements in metallic SrEuMo_{2}O_{6}

Gianluca Giovannetti, Danilo Puggioni, James M. Rondinelli, and Massimo Capone

Phys. Rev. B **93**, 115147 — Published 30 March 2016

DOI: 10.1103/PhysRevB.93.115147

Interplay between electron correlation and polar displacements in metallic $SrEuMo_2O_6$

Gianluca Giovannetti,[1,*] Danilo Puggioni,[2] James M. Rondinelli,[2,†] and Massimo Capone[1]

[1] *CNR-IOM-Democritos National Simulation Centre and International School for Advanced Studies (SISSA), Via Bonomea 265, I-34136, Trieste, Italy*

[2] *Department of Materials Science and Engineering, Northwestern University, 2220 Campus Drive, Evanston, IL 60208, USA*

Using density functional theory and dynamical mean field theory, we study the electronic properties of the proposed candidate polar metal $SrEuMo_2O_6$. Its electronic structure shares similarities with centrosymmetric $SrMoO_3$ and $EuMoO_3$, from which it may be considered an ordered derivative, but ferroelectric-like displacements of the divalent cations and oxide anions lift inversion symmetry mediated by an anharmonic lattice interaction in the metallic state. We find that Hund's coupling promotes the effects of electronic correlations owing to the Mo^{4+} d^2 electronic configuration, producing a correlated metallic phase far from the Mott state. The contraindication between metallicity and polar distortions is thereby alleviated through the renormalized quasiparticles, which are unable to fully screen the ordered local dipoles.

PACS numbers: 75.85.+t, 71.20.-b, 71.45.Gm, 77.80.B-, 78.20.Ci

I. INTRODUCTION

Noncentrosymmetric metals are an ideal playground in condensed matter physics for studying exotic phenomena and establishing new technological platforms.[1] The possible existence of these materials was theoretically discussed a half century ago,[2] but a conclusive observation of an intrinsic metallic material which undergoes an inversion-symmetry lifting (polar) transition has been obtained only recently in $LiOsO_3$.[3] The theoretical appeal of these materials lies in the contrast with one's intuition: Itinerant electrons in metals are expected to screen electric fields and flow in response to an electric field derived from an asymmetric charge density, and thus generate a distribution that cancels the field inside the metal. It is surprising then to find metals that undergo the same structural transitions that occur in isostructural and insulating analogues; it is this incompatibility, in part, that explains the scarcity of polar noncentrosymmetric metals (NCSM).

Nonetheless, polar displacements and metallicity can coexist provided that the ferroelectric-like distortions are largely decoupled from the electronic structure at the Fermi level, *i.e.*, the electrons responsible for transport.[2,7] This appears to be the main operational principle active in oxide-based NCSM: $LiOsO_3$[3] exhibits a second-order displacive transition from a non-polar to polar structure (crystal class C_{3v}) with displacements of Li and O rather than Os, whose orbitals are responsible for the metallic behavior;[8] $LaSr_2Cu_2GaO_7$ has a polar structure (C_{2v}) owing to the presence of intrinsically acentric tetrahedral GaO_4 units, whereas the conduction bandi is mainly of copper character,[9,10] and $Cd_2Re_2O_7$ is a geometrically frustrated pyrochlore that becomes optically active (D_{2d}) as oxygen rather than Re displacements lift inversion symmetry below 200 K.[11,12] A well-established noncentrosymmetric structure has been also reported in the layered ruthenate $Ca_3Ru_2O_7$.[13]

Although the framework described in Ref. 7 provides a *structural* understanding for the stability of oxide and non-oxide NCSM, it is partially limited, as it considers all metallic states equivalent assuming a Fermi liquid description. Yet, the rich phenomenology of *strongly correlated* oxides demonstrates that strong electron-electron interactions can lead to metallic states which challenge the Landau Fermi-liquid paradigm. Anomalous metallic states range from non-Fermi-liquid metals, with unconventional scaling behavior of the resistivity and other observables, to 'bad' metals that retain Fermi-liquid coherence only below a very low coherence temperature, above which the Mott-Ioffe-Regel limit breaks.[14] More recently the possibility of a 'bad metal' far from the Mott-Hubbard localization state has been proposed in the presence of a sizable Hund's coupling.[15,16] Therefore, we pose the question: How does the nature of the metallicity alter the compatibility between inversion lifting displacements and "delocalized" electrons?

We first discuss the previously mentioned NCSM oxides within this context. Indeed all may be considered to exhibit strong electron correlations. The residual resistivity in $LiOsO_3$ is larger than that expected for a normal metal and the magnetic susceptibility displays a Curie-Weiss component suggesting an incipient localization of the carriers.[3] $LaSr_2Cu_2GaO_7$ shares the same Cu-O planar structure of $YBa_2Cu_3O_7$, one of the most studied cuprate superconductors for which strong deviations from the Fermi-liquid paradigm are well established.[20] Optical studies of $Cd_2Re_2O_7$ reveal an exotic metallic state with strong mass renormalizations.[21] Lastly, $Ca_3Ru_2O_7$ has an electronic structure which resembles a mixture of metallic and insulating features[22] with strong correlation which can be associated with the Hund's exchange.[23]

Although the role of strong correlations in compounds with half-filled shells follows the longstanding Mott-Hubbard paradigm, in the presence of a sizable Hund's coupling, materials with fractional filling different from half-filling (and from one electron or hole per atom), like the d^2 configuration, display unexpected properties. These features have led to identifcation of a new class of materials dubbed "Hund's metals." Interestingly in these systems strong electron-electron correlation effects exist even for moderate values of the Hubbard repulsion, very far from the critical value of the Mott transition.[15,24] However, the extent to which the Hund's interaction can drive a correlated metallic state compatible with ferroelectric-like displacements is unknown.

In this Article, we propose $SrEuMo_2O_6$ (SEMO) as a new polar metal. We use a combination of density functional theory (DFT) and dynamical mean-field theory (DMFT)[25] to show that electron correlations (i) alter the coupling between the po-

lar ionic and metallic degrees of freedoms and (ii) reduce the screening channels, which lead to an enhancement of the polar displacements. By means of DFT calculations, we first establish that the ordered molybdate exhibits a polar metallic ground state, in which the polar displacements are decoupled to the electronic structure at the Fermi level.[7]. We then demonstrate with our DFT+DMFT approach that SEMO is in proximity to region of phase space exhibiting bad metallic behavior largely driven by the Hund's coupling owing to the d^2 electronic configuration in the Mo 4*d* manifold. Within the same approach we further show that the enhanced electron correlations that characterize the poor-metallic state reduce the ability of the metal to screen the ferroelectric-like displacements, leading to a "ferroelectric" metallic state. We demonstrate how, also in the present case, the effects of electronic correlations lead to a metallic state which is very similar to an insulator and supports the polar displacements even in such case of weak coupling between ferroelectric and metallic degrees of freedom. Our findings extend the search for yet unknown noncentrosymmetric metals to materials with electronic configurations like d^2 and d^4, where Hund's correlations are easy to establish, as opposed to Mott-Hubbard physics.

II. METHODS AND MATERIALS

We perform first-principles density functional calculations within the generalized-gradient approximation (PBE)[30] as implemented in the Vienna *Ab initio* Simulation Package (VASP)[31] with the projector augmented wave (PAW) method[32] to treat the core and valence electrons using the following electronic configurations $4s^2\ 4p^6\ 5s^2$ (Sr), $5p^6\ 6s^2$ (Eu), $4p^6\ 4d^5\ 5s^1$ (Mo),$2s^2\ 2p^4$ (O). The *f* electrons of Eu are kept frozen in our DFT calculations being localized at 2 eV below the Fermi level (E_F) in the calculations of $EuMoO_3$.[28] A kinetic cutoff energy of 550 eV is used to expand the wavefunctions and a Γ centered $10\times8\times10$ *k*-point mesh combined with the tetrahedron method is used for Brillouin zone integrations. Atomic relaxations are continued until the changes in the total energy are less than 10^{-8} eV. Variable-volume atomic relaxations are performed, relaxing the out-of-plane lattice parameter and fixing the in-plane ones to the pseudo-cubic lattice constant, $a=c=3.975$ Å.

In order to include the on-site Coulomb interaction parameterized by the Hubbard U and the Hund's coupling J_H in our DMFT calculations (we use a Kanamori parametrization), we compute maximally-localized Wannier orbitals[34] for the 4*d* Mo states over the energy range spanned by the t_{2g} orbitals across E_F to construct the non-interacting part of our Hamiltonian. In the DFT+DMFT scheme,[25] which treats the lattice problem as an impurity embedded in a self-consistent bath, we employ Exact Diagonalization (ED)[35,36] as the impurity solver using an Arnoldi algorithm[37] to perform the diagonalization. The imaginary part of the dielectric function is obtained from the DMFT optical conductivity $\sigma(\omega)$ as $\varepsilon_2(\omega)=4\pi\sigma(\omega)/\omega$, and the real part obtained via the Kramers-Kronig relation to provide the full complex dielectric function.

Cation ordering is a promising route to lift inversion symmetry and realize a NCSM.[7] Moreover, this approach is experimentally accessible through either synthetic bulk chemistry routes or heteroepitaxial thin film growth.[26,27] With this in mind, we select metallic $SrMoO_3$ (SMO) and $EuMoO_3$ (EMO) with d^2 electronic configurations and nearly identical pseudo-cubic lattice constants (a=3.975 Å).[28,29] We then construct a 1/1 period superlattice of SMO and EMO in which the Sr and Eu cations are arranged in a rock-salt structure. Spin-polarized calculations for SEMO lead to a weakly ordered ferromagnetic state such that the Mo ions exhibit a small magnetic moment of 0.17 μ_B, in contrast with the non-magnetic ground state we obtain for bulk SMO and EMO, consistent with experiment. Note that EMO is magnetic at low-temperatures owing to the Eu *f* electrons. Thus we characterize SEMO as a Pauli paramagnet, and for these reasons, we use non-spin polarized calculations throughout.

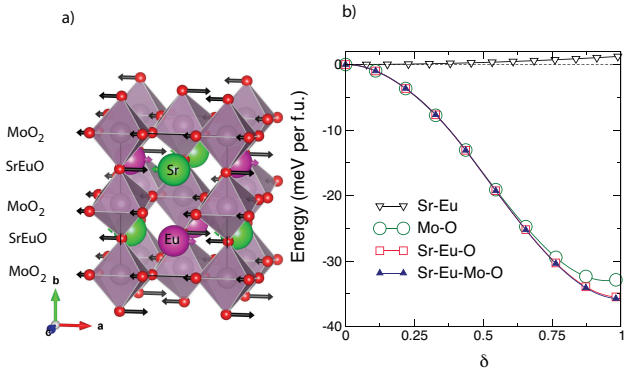

FIG. 1. Crystal structure and evolution of the energy as a function of the soft-mode distortion (δ). **a**, DFT relaxed crystal structure of $SrEuMo_2O_6$ in *Imm*2 ferroelectric crystal symmetry with polar displacements along the [100]-direction. **b**, Normalized energy gain as a function of the polar displacements given as a percentage present in the equilibrium structure (δ). Energy of the full mode is compared to that of the partial modes, where a reduced set of atoms are displaced (see legend).

TABLE I. Crystallographic parameters for the *Imm*2 ground state crystal structure of SEMO obtained within DFT-PBE.

*Imm*2 (no. 44)		$a=5.621$ Å, $b=7.983$ Å, $c=5.621$ Å		
Atom	Wyckoff Site	*x*	*y*	*z*
Sr	2*a*	0	0	0.497
Eu	2*b*	0	1/2	0.508
Mo	4*d*	0	3/4	0.
O(1)	8*e*	0.747	0.778	0.246
O(2)	2*b*	0	1/2	0.059
O(3)	2*a*	0	0	-0.048

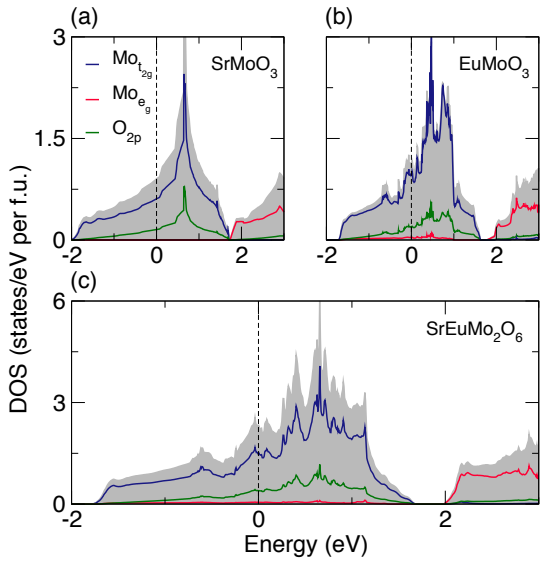

FIG. 2. Atom- and orbital-resolved resolved density-of-states (DOS) for $SrMoO_3$ **(a)**, $EuMoO_3$ **(b)**, and $SrEuMo_2O_6$ **(c)** as calculated within DFT-PBE. The Fermi level is at 0 eV (dashed line).

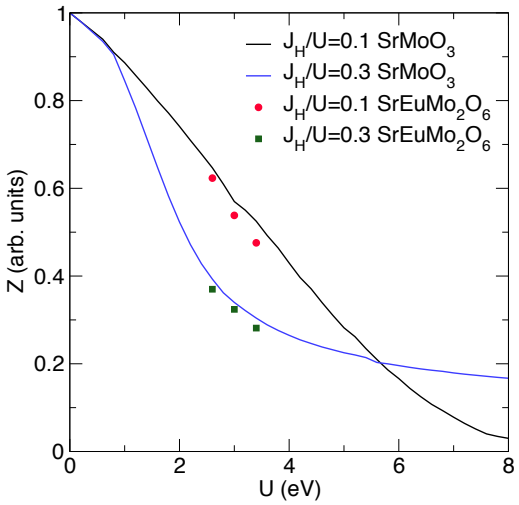

FIG. 3. Quasiparticle weights (Z) for $SrMoO_3$ and $SrEuMo_2O_6$ calculated within DFT+DMFT at different values of the ratio J_H/U.

III. RESULTS AND DISCUSSION

A. Atomic Structure

Fig. 1a depicts the polar $Imm2$ ground state crystal structure of SEMO obtained from density functional theory calculations (see Table I). This structure is 35 meV per formula unit (f.u.) lower in energy than the centric $I4/mmm$ phase. The octahedral tilt pattern of SMO and EMO is $a^0a^0a^0$ and $a^0a^0c^-$, respectively, whereas in SEMO we find the $a^-b^+a^-$ tilt with a^- and b^+ rotations of 4° and 0.11°, respectively. The loss of inversion symmetry is a consequence of the out-of-phase octahedral tilt modes which allow for anti-polar Sr and Eu cation displacements connected with neighboring O sites.[33] (Note that if the b^+ tilt amplitude is zero, the structure remains polar owing to the out-of-phase rotations that in combination with the rock salt Sr and Eu order lift inversion.) Along the polar a axis (see Fig. 1a) we find (*i*) Sr and Eu ions have opposite displacements of, respectively, 0.045, -0.018 Å (*ii*) apical O ions belonging to the same octahedra displace by 0.33 and -0.28 Å while planar O ions displace by -0.020 Å and (*iv*) Mo cations with negligible ferroelectric displacements. The situation along the non-polar b and c axes is different: the Sr, Eu and apical O ions do not displace while the planar O sites exhibit antipolar displacements.

Fig. 1b shows the variation of the total energy as a function of the amplitude δ of atomic displacements for the different atoms involved in the distortion mode connecting the $I4/mmm$ centrosymmetric structure ($\delta = 0$) to the polar $Imm2$ ground state ($\delta = 1$). We compare the total mode involving all ions (Sr-Eu-Mo-O) with three partial displacements: A-cation only mode (Sr-Eu), A-O mode (Sr-Eu-O) that includes the displacement of Sr, Eu and O atoms, and the B-O mode (Mo-O) whereby the Sr and Eu displacements are neglected. As expected, the largest energy gain (35 meV) is obtained when all atoms are included. Since the Mo cations remain largely centered in the octahedra, the results for the Mo-O mode show that the oxygen displacements are essential to the structure stability; indeed, the polar Sr-Eu displacements alone lead to an increase in energy in the absence of O displacements (Sr-Eu, Fig. 1b). The difference between the total mode and that which omits the Mo displacements (Sr-Eu-O, Fig. Fig. 1b) demonstrates that the polar ionic configuration is stabilized by cooperative and coupled displacements of the Sr, Eu and O ions. We note that among all the O atoms, the main contribution is due to apical anions found in the AO monoxide planes (Fig. 1a).

B. Electronic Properties

We now consider the electronic properties of SEMO to address the connection between the metallic state, polar displacements, and electronic screening. In Fig. 2 we compare the non-spin polarized density-of-states (DOS) calculated within DFT-PBE for bulk SMO and EMO to that of SEMO. The DOS of SMO (Fig. 2a) and EMO (Fig. 2b) are rather similar: Both bulk are found to be metallic with the extended Mo $4d$ states dispersing from approximately -2 eV to 1.8 eV above the Fermi level. Fig. 2c also shows that SEMO is metallic with sizable spectral weight at E_F. The low-energy contribution to the spectral density is dominated by bands arising from the Mo $4d^2$ electrons, which are weakly entangled with the oxygen $2p$ states mainly distributed from -8 eV to -4 eV below E_F (not shown). The $4d$ bands in SEMO have an overall width of 3.4 eV, which is close to that of EMO and reduced with respect to SMO owing to MoO_6 octahedral rotations. The narrowing of the t_{2g} manifold also separates it from the higher-lying e_g bands.

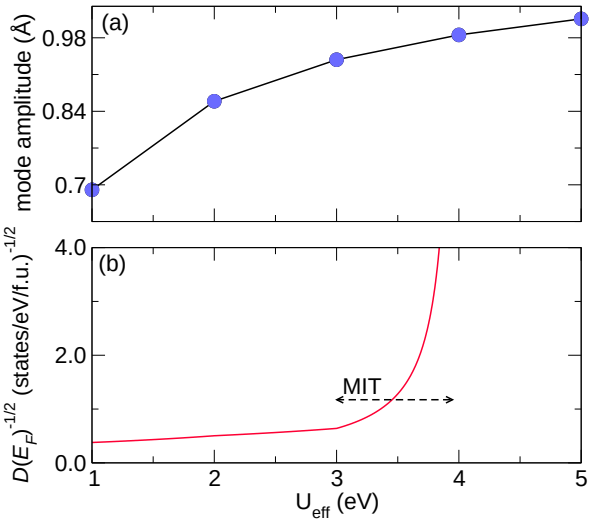

FIG. 4. Evolution in the polar mode amplitude and Thomas-Fermi screening length, $\lambda \propto 1/\sqrt{D(E_F)}$, with correlation for $SrEuMo_2O_6$.

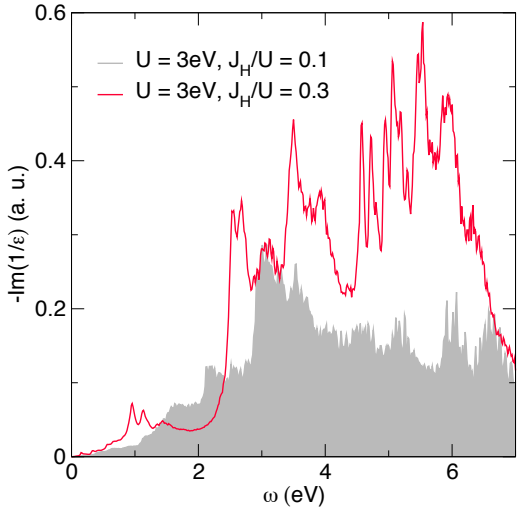

FIG. 5. Electron-energy-loss function for $SrEuMo_2O_6$.

C. Electronic Correlations and NCSM Phase Stability

Next we investigate the effect of electronic correlations in bulk centrosymmetric SMO and then compare its behavior with the polar metal SEMO. (Data for EMO is not shown because of the similarities in the results). First, we perform DMFT calculations to characterize the degree of correlation in the molybdates. We examine the quasiparticle weight Z (Fig. 3), which is 1 for a non-interacting metal and decreases as a function of the interaction strength. A vanishing Z signals a Mott insulating phase. The constrained random-phase approximation (cRPA) for bulk SMO gives $U = 3.0$ eV and $J_H = 0.3$ eV.[38] In Fig. 3 we plot Z as a function of U for two values of the ratio J_H/U ($J_H/U = 0.1$, which corresponds to the cRPA values, and 0.3). For bulk SMO with cubic symmetry the t_{2g} orbitals are perfectly degenerate and occupied by 2/3 electrons per orbital and the states share the same value of Z. For the cRPA value of $J_H/U = 0.1$, we find $Z \simeq 0.6$, consistent with experiment and previous theoretical estimates.[39]

The evolution of Z follows the behavior discussed in Ref. 24, where a rapid decrease for small U is followed by a flattening of the $Z(U)$ curve, and ultimately to a Mott transition, which occurs at a relatively large value of U ($\sim$8 eV for $J_H/U = 0.1$). This behavior is more pronounced with increasing J_H/U with a faster initial decrease and a much slower decrease to an enhanced critical strength. For the cRPA estimates, we find that SMO is indeed on the brink of a 'Hund's correlated' phase and far from the Mott state, which to achieve would require an unphysical enhancement of the ratio between U and the bare kinetic energy. Indeed, the correlated nature of the metallic state in bulk SMO is evidenced experimentally by a low quasiparticle coherence scale around $T^* = 140$ K[40], which is of the same order as Sr_2RuO_4[41] above which highly incoherent conduction characterizes the system.

Next we examine the polar metal SEMO, where the loss of inversion symmetry alters the t_{2g} manifold symmetry through a small crystal-field splitting and a change in the local hybridization. This structural effect leads to small differences between the Z values for the different orbitals. For clarity, we plot the orbital-averaged Z, and note that the reduced symmetry introduces minor modulations of the orbital occupancies without changing the physical picture. Here we observe a small reduction of the quasiparticle weight Z and consequently a slight increase of the degree of correlation (see the data plotted as circles and squares in Fig. 3), which shifts SEMO towards a correlated regime driven by the Hund's coupling. Therefore the polar metallic state of SEMO is characterized by the simultaneous presence of polar distortions and poor metallic behavior with intermediate electronic correlation strength.

The weak coupling between ferroelectric displacements and the metallic states at the Fermi level provides a way to avoid metallic screening that would normally destabilize the polar (ferroelectric) phase. Next, we establish that this weak coupling is further supported by electronic correlations. As a first step to reveal the role played by electronic correlations on the polar structure, we perform ionic relaxations as a function of the interaction strength U within the DFT+U approach where a single effective U parameter $U_{\text{eff}} = U - J$ is used. We then quantify both the low-energy electronic structure and decompose the relaxed crystal structures using a mode analysis[43] to quantify the polar displacements. We find within this scheme that SEMO behaves like a G-type antiferromagnetic metal for $U_{\text{eff}} < 3$ eV, and at larger values of U_{eff} a metal-insulator transition (MIT) occurs (see Ref. 42). In the metallic regime, Fig. 4a shows that even small changes in the electronic correlation strength alters that amplitude of the (parent-cell-normalized) polar mode depicted in Fig. 1a: As U_{eff} increases, the polar displacements also increase. Above the MIT ($U_{\text{eff}} > 3$ eV), the polar displacements grow asymptotically.

Although the weak coupling between the polar displacements and the metallic state are the origin of the stability of the polar metallic state, the electronic correlations support the polar metallic phase. This behavior can be understood as follows: First, upon increasing the correlation strength, the ionicity of the compound increases; therefore, the Mo–O bonds lose some

covalent character, promoting Sr/Eu-O interactions that result in an enhanced polar instability. Second, by approaching the MIT when entering the more correlated regime, the Thomas-Fermi screening length, $\lambda \propto 1/\sqrt{D(E_F)}$ where $D(E_F)$ is the density-of-states at the Fermi energy, increases dramatically (Fig. 4b). Fig. 5 supports this view, were we show the DMFT computed electron-energy-loss function [EELF, $-Im(1/\varepsilon)$]. On average EELF is greater in the more correlated regime ($J_H/U = 0.3$) owing to the reduced Z derived from the Hund's assisted correlations. By reducing the itinerant character of quasiparticles, the interactions driving the polar instability cannot be efficiently screened as expected in a perfect metal—the carriers behave as bare particles. Our results suggest a retarded ability of the correlated carriers to screen an electric polarization.

This observed enhancement of the polar displacements as a function of correlation strength is not a trivial result. In proper ferroelectrics, such as $BaTiO_3$ and $LiNb(Ta)O_3$, the driving mechanism behind the ferroelectric instability is due to the hybridization between the empty d-states on the transition-metal cations and the p-states on the oxide ions. Here we find that increasing the band gap, using the correlation strength U_{eff} as tuning parameter, acts to diminish the hybridization between the empty d- and p-states, resulting in the disappearance of polar displacements. This response is precisely opposite to what we find in polar metals such as SEMO, which exhibits a robust metallic state owing to partial band occupancy that does not depend on extrinsic carrier concentration.

Moreover, we emphasize that the correlated state in the polar metal SEMO is a sufficient but not a necessary condition for the stability; rather, correlations provide a synergistic contribution to the phase stability because SEMO may be classified as a type-3 NCSM according to Ref. 7. To confirm this view, we performed a computational experiment whereby we electron dope the insulating phase of SEMO at $U_{\text{eff}} = 4\,\text{eV}$. For all values of doping taken into account, the polar phase is still favored.[42] Note that in proper ferroelectrics a small amount of electronic doping destabilizes the ferroelectric instability driving the material to a paraelectric phase. Thus our results suggest that degenerately doped ferroelectrics and intrinsic noncentrosymmetric metals are unique materials classes; although some members may belong to both families, in contrast to recent suggestions[44] the driving mechanisms may be different in the presence of non-trivial correlations.

IV. CONCLUSIONS

In summary, we propose $SrEuMo_2O_6$ as a polar Hund's metal. Our electronic structure calculations reveal that the polar structure is driven by asymmetric displacements of the ions in the SrO and EuO planes. The ferroelectric-like state coexists with a correlated metallic phase which relies on the Hund's coupling and it is quite robust with respect to Mott localization despite the significant value of the Hubbard-U repulsion. The weak coupling between polar displacements and metallic states combined with electronic correlations provide the necessary interactions to stabilize the NCSM phase. Analogously to the case of U-driven strongly correlated ferroelectric metals as $LiOsO_3$, the poorly coherent quasiparticles are ineffective at completely screening the ordered local dipole moments.

Although our current understanding of polar metals reveals that many of them are likely in a correlated electronic regime with bad metallic behavior, we do not eliminate the possibility that non-correlated polar metals may exist; rather, strong electronic correlation, arising either from conventional Mott-Hubbard physics or from the relevant role of Hund's coupling, appears to be a favorable ingredient to stabilizing noncentrosymmetric metallic phases, but it may not be a prerequisite in scenarios where the inversion lifting displacements are indeed fully decoupled from the low-energy electronic structure.

These results strengthen the link between correlated metallic states and the propensity of a metallic material to adopt polar structure, facilitating the selection or design of new correlated polar metals for enhanced magnetoelectronic responses or customized antisymmetric exchange interactions, which support exotic magnetic textures (helical or skyrmionic structures). The present work also extends the candidate materials to electronic configurations which are not particularly favorable for Mott localization but are sensitive to the Hund's coupling. For example, our results suggest that materials with d^2 electronic configurations are promising candidates from which to realize new polar metals. Provided ferroelectric-like displacements can be realized through a lattice instability or anharmonic mode interactions,[45] poor screening of the electric dipoles will be provided in the correlated metallic state when the Hund's coupling is sufficiently large. An interesting example could be given by $LiReO_3$, which displays the same polar crystal class as $LiOsO_3$ ($R3c$)[46] owing to the off-centering of Li ions, while it shares the same nominal d^2 electronic configuration of SEMO.

ACKNOWLEDGMENTS

G.G. and M.C. acknowledge financial support from the European Research Council under FP7/ERC Starting Independent Research Grant "SUPERBAD" (Grant No. 240524). D.P. and J.M.R. acknowledge the Army Research Office for financial support (Grant No. W911NF-15-1-0017), and the HPCMP of the DOD and XSEDE supported by NSF (Grant No. OCI-1053575) for providing computational resources.

* ggiovann@sissa.it
† jrondinelli@northwestern.edu

[1] V. Keppens, Nat. Mater. **12**, 952 (2013).
[2] Anderson and Blount , Phys. Rev. Lett. **14**, 217 (1965).
[3] Y. Shi, Y. Guo, X. Wang, A. J. Princep, D. Khalyavin, P. Manuel, Y. Michiue, A. Sato, K. Tsuda, S. Yu, M. Arai, Y. Shirako, M. Akaogi, N. Wang, K. Yamaura and A. T. Boothroyd , Nat. Mater. **12**, 1024 (2013).

[4] W. Cochran, Adv. Phys., 9 (1960) 387.
[5] X. Gonze, J.-C Charlier , D. C. Allan and M. P. Teter, Phys. Rev. B, 50 (1994) 13035.
[6] Ph. Ghosez, X. Gonze and J.-P. Michenaud, Europhys. Lett. 33 713 (1996).
[7] D. Puggioni and J. M. Rondinelli, Nat. Commun. **5**, 3432 (2014).
[8] G. Giovannetti and M. Capone, Phys. Rev. B **90**, 195113 (2014).
[9] K. Poeppelmeier, J. Thiel, J. Vaughey, M. Anderson, M., D. Groenke, C. Stern, B. Dabrowski, D. Hinks and A. Mitchell, Physica C: Superconductivity 185, Part 1, 525 (1991).
[10] J. T. Vaughey, J. P. Thiel, E. F. Hasty, D. A. Groenke, C. L. Stern, K. R. Poeppelmeier, B. Dabrowski, D. G. Hinks and A. W. Mitchell, Chem. Mat. 3, 935 (1991).
[11] A. Sergienko, V. Keppens, M. McGuire, R. Jin, J. He, S. H. Curnoe, B. C. Sales, P. Blaha, D. J. Singh, K. Schwarz, and D. Mandrus, Phys. Rev. Lett. **92**, 065501 (2004).
[12] J. C. Petersen, M. D. Caswell, J. S. Dodge, I. A. Sergienko, J. He, R. Jin and D. Mandrus, Nat. Phys. **2**, 605 (2006).
[13] Y. Yoshida, S. Ikeda, H. Matsuhata, N. Shirakawa, C. H. Lee, and S. Katano , Phys. Rev. B **72**, 054412 (2005).
[14] X. Deng, J. Mravlje, R. Zitko, M. Ferrero, G. Kotliar, and A. Georges, Phys. Rev. Lett. 110, 086401 (2013)
[15] A. Georges, L. de' Medici, and J. Mravlje, Annu. Rev. Condens. Matter Phys. **4** 137 (2011).
[16] K. Haule and G. Kotliar, New J. Phys. **11**, 025021 (2009)
[17] Y. Wang, X. Liu, J. D. Burton, S. S. Jaswal, and E. Y. Tsymbal, Phys. Rev. Lett. **109**, 247601 (2012).
[18] T. Kolodiazhnyi, M. Tachibana, H. Kawaji, J. Hwang, and E. Takayama-Muromachi, Phys. Rev. Lett. **104**, 147602 (2010).
[19] J. Hwang, T. Kolodiazhnyi, J. Yang, and M. Couillard, Phys. Rev. B **82**, 214109 (2010).
[20] N. Trivedi and M. Randeria, Phys. Rev. Lett. **75**, 312 (1995).
[21] N. L. Wang, J. J. McGuire, T. Timusk, R. Jin, J. He, and D. Mandrus, Phys. Rev. B **66**, 014534 (2002).
[22] G. Cao, L. Balicas, Y. Xin, E. Dagotto, J. E. Crow, C. S. Nelson, and D. F. Agterberg, Phys. Rev. B **67**, 060406(R) (2003).
[23] J. Mravlje, M.Aichhorn, T. Miyake, K. Haule, G. Kotliar, and A. Georges, Phys. Rev. Lett. **106**, 096401 (2011).
[24] L. de' Medici, J. Mravlje, and A. Georges, Phys. Rev. Lett. **107**, 256401(2013).
[25] A. Georges, G. Kotliar, W. Krauth, and M. J. Rozenberg, Rev. Mod. Phys. **68**, 13 (1996).
[26] G. King, P. M. Woodward, J. Mater. Chem. **20**, 5785 (2010); W. Dachraoui, T. Yang, C. Liu, G. King, J. Hadermann, G. Van Tendeloo, A. Llobet, A. and M. Greenblatt, Chem. Mat. **23**, 2398 (2011).
[27] P. Zubko, S. Gariglio, M. Gabay, P. Ghosez, J. M. Triscone, Annu. Rev. Condens. Matter Phys. 2, 141 (2011).
[28] Y. Kozuka, H. Seki, T. C. Fujita, S. Chakraverty, K. Yoshimatsu, H. Kumigashira, M. Oshima, M. S. Bahramy, R. Arita, and M. Kawasaki, Chem. Mater., **24**, 3746 (2012).
[29] R. B. Macquart, B. J. Kennedy, and M. Avdeev, J. Solid State Chem. **183**, 249 (2010).
[30] J. P. Perdew, K. Burke, and M. Ernzerhof, Phys. Rev. Lett. **77**, 3865 (1996).
[31] G. Kresse and J. Hafner, Phys. Rev. B, **47** ,558 (1993); G. Kresse and J. Hafner, Phys. Rev. B, **49**, 14251 (1994); G. Kresse and J. Furthmuller, Comput. Mat. Sci., **6**, 15 (1996); G. Kresse and J. Furthmuller, Phys. Rev. B **54**, 11169 (1996).
[32] P. E. Blöchl, Phys. Rev. B **50**, 17953 (1994); G. Kresse and D. Joubert, Phys. Rev. B **59**, 1758(1999).
[33] J. Young and J. M. Rondinelli, Chem. Mater. **25**,4545 (2013).
[34] A. A. Mostofi, J. R. Yates, Y.-S. Lee, I. Souza, D. Vanderbilt and N. Marzari, Comput. Phys. Commun. **178**, 685 (2008).
[35] M. Caffarel and W. Krauth, Phys. Rev. Lett. **72**, 1545 (1994).
[36] M. Capone, L. de' Medici, and A. Georges, Phys. Rev. B **76**, 245116 (2007).
[37] R. B. Lehoucq, D. C. Sorensen, and C. Yang, ARPACK Users Guide (SIAM, Philadelphia, 1997).
[38] L. Vaugier, H. Jiang, and S. Biermann, Phys. Rev. B **86**, 165105 (2012).
[39] H. Wadati, K. Yoshimatsu, H. Kumigashira, M. Oshima, T. Sugiyama, E. Ikenaga, A. Fujimori, J. Mravlje, A. Georges, A. Radetinac, K. S. Takahashi, M. Kawasaki, Y. Tokura, Phys. Rev. B **90**, 205131 (2014).
[40] I. Nagai, N. Shirakawa, S-I. Ikeda, R. Iwasaki, H. Nishimura and M. Kosaka, Appl. Phys. Lett. **87**, 024105 (2005).
[41] S.-C. Wang, H.-B. Yang, A. K. P. Sekharan, H. Ding, J. R. Engelbrecht, X. Dai, Z. Wang, A. Kaminski, T. Valla, T. Kidd, A. V. Fedorov, and P. D. Johnson, Phys. Rev. Lett. **92**, 137002 (2004).
[42] See Supplemental Material at [URL will be inserted by publisher] for the effect of U and electron doping on the metallic and polar state of $SrEuMo_2O_6$.
[43] J. M. Perez-Mato, D. Orobengoa, and M. I. Aroyo, Acta Crystallographica Section A **66**, 558 (2010).
[44] N. A. Benedek and T. Birol, J. Mater. Chem. C, Advance Article (2016). DOI: 10.1039/C5TC03856A.
[45] J. Young, A. Stroppa, S. Picozzi, J.M. Rondinelli, J. Phys.: Condens. Matter **27**, 283202 (2015).
[46] R.J. Cava, A. Santoro, D.W. Murphy, S.M. Zahurak, R.S. Roth, J. Solid State Chem. **42**, 251 (1982).